Chiral Mesoporous Organosilica Nanospheres: Effect of Pore Structure on the Performance in Asymmetric Catalysis

Xiao Liu,[a, b] Peiyuan Wang,[a] Lei Zhang,[a] Jie Yang,[a] Can Li,*[a] and Qihua Yang*[a]

Abstract: (R)-(+)-1,1′-Bi-2-naphthol ((R)-(+)-Binol)-functionalized (Binol = 2,2′-dihydroxy-1,1′-binaphthyl) chiral mesoporous organosilica nanospheres with uniform particle size (100 to 300 nm) have been synthesized by co-condensation of tetraethoxysilane and (R)-2,2′-di(methoxymethyl)oxy-6,6′-di(1-propyl trimethoxysilyl)-1,1′-binaphthyl in a basic medium with cetyltrimethylammonium bromide as the template. Nanospheres with a radiative 2D hexagonal channel arrangement exhibit higher enantioselectivity and turnover frequency than those with a penetrating 2D hexagonal channel arrangement (94 versus 88% and 43 versus 15 h^{-1}, respectively) in the asymmetric addition of diethylzinc to aldehydes. In addition, under similar conditions, the enantioselectivity of the nanospheres can be greatly improved as the structural order of the framework increases. These results clearly show that the structural order of nanospheres affects enantioselective reactions. The enantioselectivity of the nanospheres synthesized by the co-condensation method is higher than that of nanospheres prepared by a grafting method and even higher than that of their homogeneous counterpart. These results indicate that the bite angle of (R)-(+)-Binol bridging in a more rigid porous network is in a more favorable position for achieving higher enantioselectivity. The efficiency of a co-condensation method for the synthesis of high-performance heterogeneous asymmetric catalysts is also reported.

Keywords: asymmetric catalysis · binol derivatives · mesoporous materials · nanoparticles · organosilica

Introduction

Since the first report of mesoporous silicas by Mobil scientists in the 1990s, much research effort has been devoted to the controllable synthesis of mesoporous silicas with different framework component, mesoporous structure, and external morphology, which play important roles in the versatile application of the mesoporous silicas.[1,2] To date, mesoporous silicas with various morphologies, such as spheres,[3]

[a] Dr. X. Liu,⁺ Dr. P. Wang,⁺ Dr. L. Zhang, Dr. J. Yang, Prof. Dr. C. Li, Prof. Dr. Q. Yang
State Key Laboratory of Catalysis
Dalian Institute of Chemical Physics
Chinese Academy of Sciences
457 Zhongshan Road, Dalian 116023 (China)
Fax: (+86) 411-84694447
E-mail: canli@dicp.ac.cn
   yangqh@dicp.ac.cn

[b] Dr. X. Liu⁺
Graduate School of the Chinese Academy of Sciences
Beijing 100049 (China)

[⁺] These authors contributed equally to this work.

💻 Supporting information for this article is available on the WWW under http://dx.doi.org/10.1002/chem.201000931.

films,[4] hollow spheres,[5] hollow tubes,[6] rods,[1,7] monoliths,[8,9] helical structures,[10] and vesicles,[11] have been successfully synthesized. For many applications, increasing the diffusion rate of the guest molecule and the exposed number of active sites can greatly improve the performance of the mesoporous silicas. Generally, several approaches are employed to meet this demand, such as generating a hierarchical porous structure in mesoporous silicas,[9,12] decreasing the particle size of mesoporous silicas to the nanoscale,[13] and so on.

As an important branch of mesoporous materials, the periodic mesoporous organosilicas (PMOs) synthesized from bridged silane precursors, (R′O)₃Si-R-Si(OR′)₃, have attracted much research attention because of their unique properties (such as high mechanical and hydrothermal stability, and tunable surface hydrophilicity/hydrophobicity) derived from the uniformly distributed organic moieties (ethylene, thiophene, biphenylene, ferrocene, etc.) in the mesoporous framework.[14] Driven by the ever-increasing demand for nonracemic chiral chemicals, the synthesis of chiral PMOs with a chiral ligand bridged in the framework is very interesting because the development of chiral porous materials is one of the key subjects in asymmetric catalysis. The PMOs with chiral ligands in the framework, such as VO(salen)

(salen = 2,2′-ethylenebis(nitrilomethylidene)diphenol),[15] *trans*-diaminocycloxene,[16] and ʟ-tartardiamide,[17] have been successfully synthesized and used for asymmetric catalysis. However, they generally show lower activity and enantioselectivity than their homogeneous counterparts, which is also one of the major obstacles for their use in heterogeneous asymmetric catalysis. Engineering the mesostructural ordering and morphology of the chiral PMOs may be very important for achieving high enantioselectivity and catalytic activity. For example, previous studies demonstrated that the pore wall rigidity has a big influence on the chiral inducibility of the chiral PMOs. It has also been shown that the catalytic activity of the mesoporous silicas can be greatly improved by decreasing the particle size to the nanoscale, because of the short diffusion lengths as a result of the nanoparticle size.[18] However, control of the mesostructural ordering and morphology of the chiral PMOs is very difficult, and the synthesis of chiral PMOs with nanospherical morphology has been seldom reported.

Herein, we report the synthesis of chiral mesoporous organosilica nanospheres with (*R*)-(+)-1,1′-bi-2-naphthol ((*R*)-(+)-Binol) bridged in the framework (Scheme 1). The effects
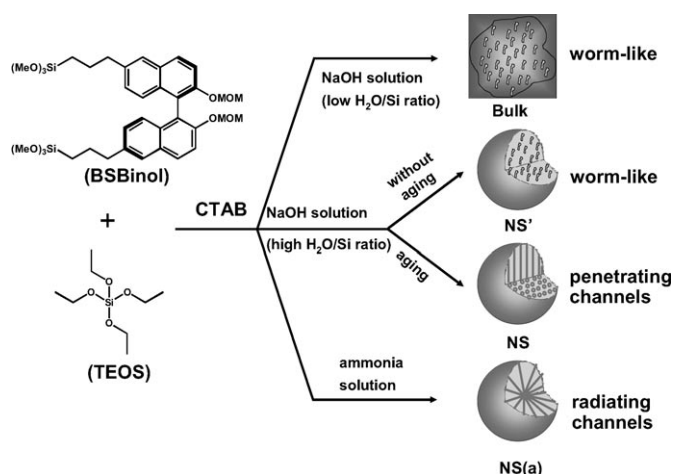
Scheme 1. Synthesis of (*R*)-(+)-Binol-functionalized chiral PMO nanospheres with different pore structures. MOM: methoxymethyl ether; CTAB: cetyltrimethylammonium bromide; TEOS: tetraethoxysilane; NS, NS′, and NS(a): different types of nanospheres.

of the synthesis medium (pH value and base source), mesostructural ordering, and morphology on the catalytic performance of the resultant materials were investigated. The asymmetric addition of diethylzinc to aldehydes was chosen as a model reaction to test the catalytic properties of the chiral nanospheres (coordinated with Ti(O*i*Pr)₄).

Results and Discussion

Structure and morphology characterization of the chiral mesoporous organosilicas: Recently, our group reported the synthesis of chiral mesoporous organosilicas with (*R*)-(+)-

Binol bridging in the framework by using a mixture of (*R*)-2,2′-di(methoxymethyl)oxy-6,6′-di(1-propyl-trimethoxysilyl)-1,1′-binaphthyl (BSBinol) and 1,2-bis(trimethoxysilyl)ethane or tetramethoxysilane as precursor and P123 as surfactant under acid conditions.[19] In this work, we synthesized chiral mesoporous organosilicas under different basic conditions to investigate the effects of pore structure on the catalytic performance. A NaOH aqueous solution (0.2 M) was first employed for the synthesis of a chiral mesoporous organosilica sample denoted Bulk. The TEM image shows that sample Bulk has an irregularly shaped morphology with a particle size larger than 5 μm (Figure 1). The XRD pattern of this
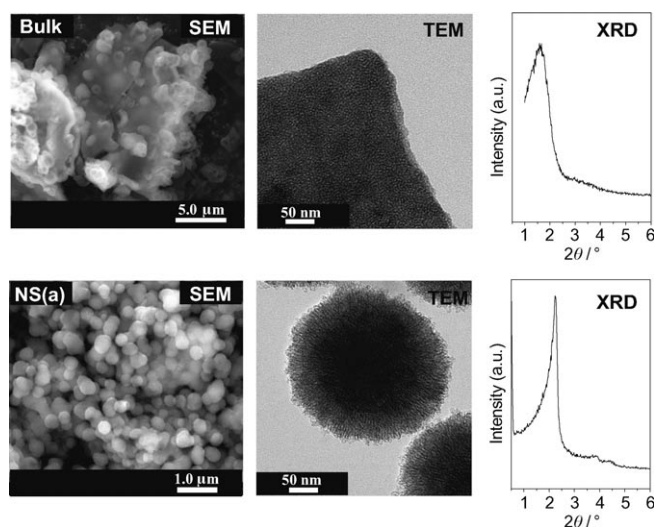

Figure 1. SEM images, TEM images, and XRD patterns of the (*R*)-(+)-Binol-functionalized mesoporous organosilicas Bulk and NS(a), which were synthesized in NaOH aqueous solution with low H₂O/Si ratio and in ammonia solution, respectively.

sample displays a broad diffraction peak at 2θ of 1.6°, characteristic of the mesoporous materials with wormhole-like mesoporous structure (Figure 1).[20] The TEM image of this sample clearly shows the existence of wormhole-like pores throughout the sample, further confirming the XRD result (Figure 1).

Previous studies showed that the nanospheres can be formed under basic conditions with high H₂O/Si molar ratio.[21] Therefore, the NS and NS′ samples (Scheme 1) were synthesized in the presence of a large amount of water. The SEM images of NS and NS′ show that the materials are both composed of nanospheres with particle size 100 to 150 nm, which suggests that the hydrothermal treatment process has no obvious influence on the morphology (Figure 2). NS′ shows one broad diffraction peak together with a shoulder in the XRD pattern. From further TEM characterization, NS′ has a wormhole-like porous structure similar to that of Bulk but with a higher degree of ordering (Figure 2). Three well-defined XRD peaks, which can be assigned to the (100), (110), and (200) diffractions of a highly ordered *P6mm* mesophase, appear in the XRD pattern of
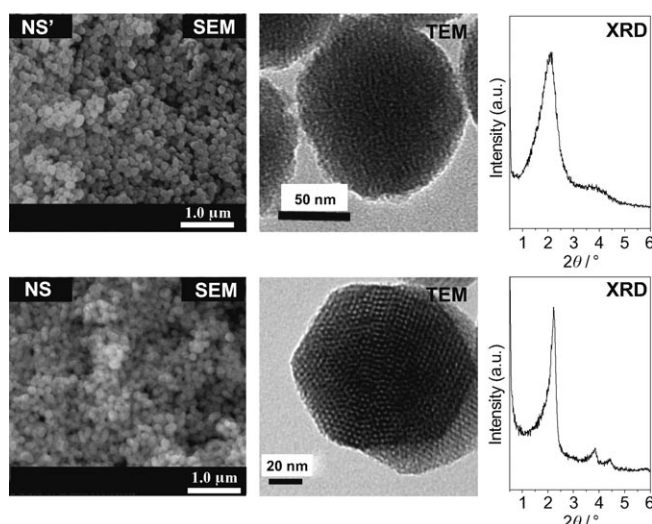
Figure 2. SEM images, TEM images, and XRD patterns of the (R)-(+)-Binol-functionalized mesoporous organosilicas NS′ and NS, which were synthesized in NaOH aqueous solution with high H_2O/Si ratio without and with aging, respectively.

NS (Figure 2).[22] Straight, parallel channels together with honeycomb mesopores penetrate throughout the TEM images of the nanospheres (Figure 2). The TEM and XRD characterizations show that NS has a more ordered meso-structure than NS′. The above results suggest that the hydro-thermal treatment favors the formation of a highly ordered mesoporous structure.

Through increasing the H_2O/Si ratio, mesoporous nano-spheres can be easily formed. Rather than NaOH, ammonia is generally used for the preparation of silica nanoparticles by Mou's group.[23] Therefore, ammonia solution was also used for the synthesis of chiral mesoporous organosilica nanospheres. NS(a) is composed of nanospheres with parti-cle size in the range of 250 to 300 nm (Figure 1). Compared with NS samples, the particle size of NS(a) is larger. The structural order of NS(a) was further characterized by XRD (Figure 1). Three well-resolved diffraction peaks, indexed to the (100), (110), and (200) peaks of a highly ordered $P6mm$ mesophase, were clearly observed in the XRD pattern of NS(a), thus showing that this material has a 2D hexagonal mesostructure. The TEM image of NS(a) exhibits striations radiating from the center of the nanospheres (Figure 1). To our knowledge, this is the first report of the synthesis of chiral mesoporous organosilica nanospheres with radiative 2D hexagonal channels.

From the above characterizations, it can be concluded that nanospheres with a wormhole-like or 2D hexagonal mesostructure can be controllably synthesized in basic medium without and with hydrothermal treatment, respec-tively. Though NS(a) and NS have a similar structural order, the channel orientation of these two materials is different. NS(a) synthesized in ammonia solution has channels radiat-ing from the center of the nanosphere and NS synthesized in NaOH solution has straight channels penetrating from one pole to the other. As we know, the structure and mor-

phology of the mesoporous materials were greatly affected by the pH of the synthesis medium and the organic addi-tives. Therefore, mesoporous organosilicas with different morphology and mesostructure could be obtained by adjust-ing the pH value of the synthesis medium and by the addi-tion of organic additives.

The nitrogen sorption isotherms of Bulk, NS′, NS, and NS(a) are of type IV with a sharp capillary condensation step in the relative pressure P/P_0 of 0.2 to 0.4, which shows that all the materials have mesopores (Figure 3). The physi-
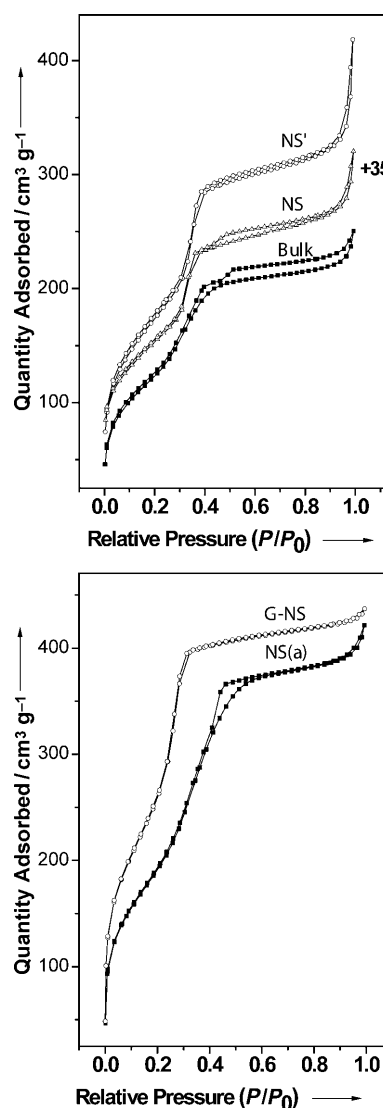

Figure 3. Nitrogen sorption isotherms of (R)-(+)-Binol-functionalized mesoporous organosilicas synthesized under different conditions.

cal parameters of the materials are summarized in Table 1. NS(a) has the largest Brunauer–Emmett–Teller (BET) sur-face area among the nanospheres. NS′ has a higher BET sur-face area and pore volume than NS, probably due to frame-work contraction during the hydrothermal treatment pro-cess. All the nanospheres have a similar pore diameter (2.4–

Table 1. Physicochemical properties of (R)-(+)-Binol-functionalized mesoporous organosilicas.

| Sample	d spacing [nm]	BET surface area [m²g⁻¹]	Pore volume [cm³g⁻¹]	Pore diameter[a] [nm]	Wall thickness[b] [nm]
Bulk	5.5	460	0.39	2.5	–
NS′	4.1	639	0.64	2.6	–
NS	4.0	444	0.44	2.4	2.2
NS(a)	3.9	722	0.65	2.4	2.1
G-NS	4.0	796	0.52	2.1	2.5

[a] Calculated using the Barrett–Joyner–Halenda (BJH) model on the adsorption branch of the isotherm. [b] Calculated by a_0−pore diameter, where $a_0 = 2d_{100}/\sqrt{3}$.

2.6 nm) and pore wall thickness (2.1–2.2 nm). Bulk shows similar BET surface area, pore volume, and pore diameter to those of NS.

For comparison, sample G-NS was also prepared by grafting of BSBinol onto mesoporous silica nanospheres. G-NS shows a similar XRD pattern and TEM image to those of NS(a), which suggests that G-NS also has a 2D hexagonal mesostructure (see the Supporting Information). The nitrogen sorption isotherm of the G-NS material is of type IV with a BET surface area of 796 cm³g⁻¹ and pore diameter of 2.1 nm (Table 1 and the Supporting Information).

Composition characterization of the chiral mesoporous organosilica nanospheres: The content of the chiral moiety in the mesoporous materials was characterized by C, H, and N elemental analysis (Table 2). The (R)-(+)-Binol content in G-NS, NS′, NS, Bulk, and NS(a) was 0.56, 0.94, 0.69, 0.36,

and 0.57 mmol g⁻¹, respectively. Bulk synthesized in the strongest basic medium had the lowest organic content among the four samples, which suggests that the strong basic conditions are not favorable for the incorporation of an organic functionality into the mesoporous materials.[24] NS′ had a much higher organic content than NS; this is probably due to the removal of loosely cross-linked organic functionality during the hydrothermal treatment process. G-NS prepared by a grafting method had an (R)-(+)-Binol content of 0.56 mmol g⁻¹, which is comparable to that of NS(a).

The FTIR spectra of the Bulk, NS′, NS, and NS(a) materials show the characteristic bands of CH₂ for aliphatic C–H stretching vibrations at 3000–2900 cm⁻¹ (see the Supporting Information). The bands at 1466, 1400, and 1385 cm⁻¹ can be ascribed to the vibrations of the aromatic ring of the Binol group. The FTIR characterization shows the successful incorporation of (R)-(+)-Binol onto the mesoporous nanospheres.

To further confirm the incorporation of (R)-(+)-Binol moieties in PMOs, the materials were characterized by ¹³C cross-polarization magic-angle spinning (CP/MAS) NMR and ²⁹Si MAS NMR spectroscopy (Figure 4). In the ¹³C CP/MAS NMR spectrum of the characteristic NS(a), the signals in the range of 160–110 ppm were ascribed to aryl carbon atoms of (R)-(+)-Binol. The signals at 46.8, 26.3, and 16.1 ppm could be assigned to C³, C², and C¹ carbon species

Table 2. Ti-promoted asymmetric addition of diethylzinc to benzaldehyde on chiral mesoporous organosilicas.[a]
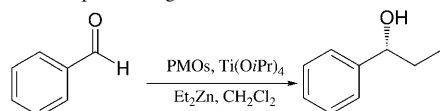
Catalyst	Time [h]	Conversion[b] [%]	ee[b] [%]	TOF[c] [h⁻¹]	Binol content[d] [mmol g⁻¹]	Binol content[d] [mmol m⁻²]
G-NS	6	95	76	6	0.56	0.5 × 10⁻³
NS′	6	86	61	5	0.94	1.4 × 10⁻³
NS	6	99	88	15	0.69	1.6 × 10⁻³
Bulk	6	36	33	1	0.36	0.8 × 10⁻³
NS(a)	2	99	94	43	0.57	0.8 × 10⁻³
PBT-10[e]	4	99	91	22	0.29	0.5 × 10⁻³
(R)-(+)-Binol	1	99	87	69	–	–

[a] All the reactions were carried out in CH₂Cl₂ with Ti(OiPr)₄ (1.5 mmol), Et₂Zn (3.0 mmol), and benzaldehyde (1.0 mmol) at 0°C. The molar ratio of Ti to ligand was 13. [b] Conversions and ee values were determined by GC on an HP-Chiral 19091G-B213 capillary column. [c] TOF was calculated according to the following equation: TOF = mmol_converted benzaldehyde/(mmol_Binol × h). [d] Determined by elemental analysis based on the C contents. [e] PBT-10 is the material synthesized by co-condensation of BSBinol and tertramethoxysilane in acidic medium using P123 as surfactant.[19]
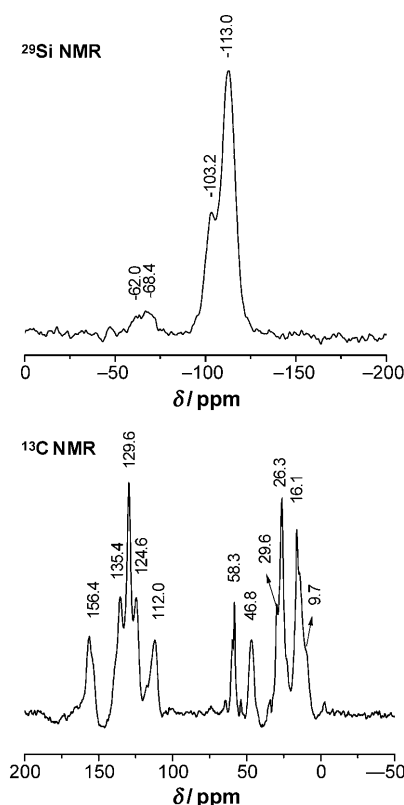

Figure 4. ²⁹Si MAS NMR and ¹³C CP/MAS NMR spectra of (R)-(+)-Binol-functionalized organosilica nanospheres NS(a), which were synthesized in ammonia solution.

of Si-C^{1}H$_2$C^{2}H$_2$C^{3}H$_2$, respectively. The absence of signals at 55.9 and 95.0 ppm shows that the protecting groups (MOM) can be removed during the process of surfactant extraction. The signals centered at 58.3 and 16.1 ppm (overlapped with the signal of C^1) may originate from the ethoxy groups formed during the surfactant-extraction process. The weak signals at 64.5, 54.0, 29.6, and 9.7 ppm (overlapped with the signal of ethoxy groups during the surfactant-extraction process) may originate from the residual surfactant. The ^{13}C CP/MAS NMR characterization confirms the incorporation of organic groups in the mesoporous materials.

The ^{29}Si MAS NMR spectrum of NS(a) shows both the T and Q silicon sites. The broad signal in the range of −50 to −80 ppm is for silicon species connected with the organic group. The signals at −113.0 and −103.2 ppm arise from the Si species Q^4 (Si(OSi)$_4$) and Q^3 (Si(OH)(OSi)$_3$), respectively. The results of NMR spectroscopy further prove that the organic group was incorporated in the mesoporous network, which is consistent with the results of FTIR spectroscopy.

The direct determination of the enantiomeric purity of (R)-(+)-Binol in the mesoporous organosilicas is very difficult. Hence, we used NaOH (1 M) to dissolve the mesoporous organosilica and characterized the resultant solution by circular dichroism (CD). The CD curve of (R)-(+)-Binol (see the Supporting Information) showed a negative Cotton effect centered in the range of 220–270 nm. The solution of Bulk, NS′, NS, and NS(a) also showed the same negative Cotton effect centered in the range of 220–270 nm. The results implied that there was almost no change in the chirality of the (R)-(+)-Binol groups during the synthesis.

To identify the location of (R)-(+)-Binol groups in PMOs clearly, we used Fe(OAc)$_2$ to coordinate with (R)-(+)-Binol in NS(a) and G-NS. After coordination, the samples were analyzed by scanning transmission electron microscopy (STEM) and energy-dispersive X-ray spectrometry (EDX) with high-resolution transmission electron microscopy (HRTEM; see the Supporting Information). Figure S-4 in the Supporting Information displays the STEM image and Fe mapping of the chosen area by using EDX. The white dots represent the signal of Fe, which has a uniform distribution in NS(a). On the contrary, the signal of Fe in G-NS has an irregular distribution and is spread mainly around the rim of the nanosphere. The results of Fe mapping suggest that the co-condensation method can lead to PMOs with a more uniform distribution of (R)-(+)-Binol groups than the grafting method.

Catalytic performance of the nanospheres: (R)-(+)-Binol can efficiently catalyze the asymmetric addition of dialkyl zinc to aldehydes, which is one of the most important asymmetric C−C bond formation reactions for the production of pharmaceutically useful chiral secondary alcohols. Because of the advantages of heterogeneous asymmetric catalysis, such as easy separation and recycling of the catalyst, the chiral Binol has been immobilized onto many kinds of solid supports.[25] Mesoporous silicas are promising solid supports because of their high surface area and ordered pore arrange-

ment. However, only a few papers have reported the use of mesoporous silica nanospheres as a solid support for asymmetric catalysis.[26]

Table 2 summarizes the surface coverage of (R)-(+)-Binol and the catalytic performance of the materials in the Ti-promoted asymmetric addition of diethylzinc to benzaldehyde; the reaction profiles are displayed in Figure 5. G-NS synthe-
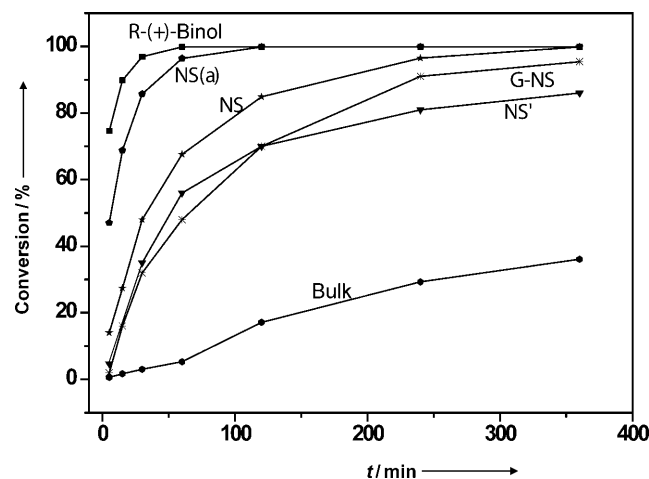

Figure 5. Reaction time profiles of Ti-promoted asymmetric addition of diethylzinc to benzaldehyde on different kinds of catalysts.

sized by a grafting method can efficiently catalyze the Ti-promoted asymmetric addition of diethylzinc to benzaldehyde. Within 6 h, the conversion of benzaldehyde can reach 95%. However, it takes only 1 h for the homogeneous counterpart to fully convert the benzaldehyde. An enantiomeric excess (ee) value of 76% was obtained on G-NS, which is slightly lower than that with homogeneous (R)-(+)-Binol (87% ee) under identical reaction conditions. The decreasing of the ee value was also observed for solid catalysts prepared by grafting (R)-(+)-Binol onto unmodified porous silica.[25] The turnover frequency (TOF) of G-NS and (R)-(+)-Binol is 6 and 69 h^{-1}, respectively. The much lower TOF of G-NS is probably due to the irregularly distributed (R)-(+)-Binol on the mesoporous silica, which makes the access of the substrate to the active site difficult. Compared with the grafting method, the co-condensation method favors the formation of mesoporous silicas with uniformly distributed organic groups, which may provide a chance to increase the ee value and catalytic activity of the solid catalysts by increasing the homogeneity of (R)-(+)-Binol.

NS′ and NS synthesized by the co-condensation method were tested in the same reaction. Under similar reaction conditions, it is surprising to find that NS′ and NS with similar morphology show quite different catalytic performance. Conversions of 86% with 61% ee and of 99% with 88% ee were obtained on NS′ and NS, respectively, within 6 h. Calculated from the reaction profile, the TOF of NS is three times that of NS′. The above characterizations show that NS′ has a much higher BET surface area and pore volume

but less structural order than NS. Also, the surface coverage of (R)-(+)-Binol on NS′ is comparable to that on NS. The much lower *ee* value and TOF of NS′ than of NS can only be assigned to their different structural order and pore wall rigidity. It is reported that the bite angle of (R)-(+)-Binol determines the enantioselectivity of asymmetric reactions.[27] It is also generally accepted that the hydrothermal treatment process increases the cross-linking degree of the network. NS has more rigid pore walls than NS′. Thus, the catalytic performance of the PMOs may be influenced by the structural order of the materials. In this case, it seems that the *ee* value and TOF can be greatly accelerated by increasing the structural order from a wormhole-like to 2D-ordered mesostructure.

To further elucidate the role of the structural order in the catalytic performance of the chiral PMOs, Bulk and NS(a) prepared with hydrothermal treatment were also tested in the Ti-promoted asymmetric addition of diethylzinc to benzaldehyde (Table 2). Bulk has a less ordered wormhole-like structure than NS′ from the above characterizations. Within 6 h, the conversion can only reach 36% with 33% *ee*. The TOF of Bulk is only 1 h^{-1}. The catalytic activity and *ee* value of Bulk are much lower than those of NS′. The low catalytic activity of Bulk can be explained by the large particle size and low BET surface area, which do not favor the fast diffusion of guest molecules throughout the mesoporous matrix during the catalytic process. The reason for the low enantioselectivity is probably the less ordered pore structure.

NS(a) with an ordered and radiative mesoporous structure shows a TOF of 43 h^{-1} with 94% *ee*, which is the highest among all the PMOs investigated and even higher than that of the material which we synthesized under acidic conditions (Table 2, PBT-10).[19] The *ee* value of NS(a) is even higher than that of the homogeneous catalyst under similar reaction conditions. The higher TOF observed for NS(a) is partly due to the higher surface area and pore volume and partly due to the radiative arrangement of the pore channels. Furthermore, NS(a) with radiating channels has a higher activity and enantioselectivity than NS with penetrating channels. This is probably due to the combined effect of the bite angle of the Binol in the PMOs and the rigidity of the mesoporous framework.

Based on the above results, it could be summarized that the chiral PMOs with ordered mesostructure (NS and NS(a)) show higher enantioselectivity than that of the disordered wormlike mesostructure (NS′ and Bulk). Also, the chiral PMOs synthesized by the co-condensation method are more enantioselective than the catalyst made by the grafting method. The enantioselectivity of the chiral PMOs derives from the (R)-(+)-Binol bridging in the mesoporous network. It has been previously reported that the bite angle of the binaphthalene chiral building block determines the enantioselectivity.[27] By use of a bridged silane precursor for the synthesis of PMOs, the organic groups should be dispersed both in the network and on the surface. Therefore, the structural order may influence the orientation of the organic group in the network or on the surface. Moreover, the

bite angle of (R)-(+)-Binol may also be affected by the rigidity of the PMOs. Therefore, it could be proposed that a more ordered mesostructure and rigid pore wall favors the bite angle of (R)-(+)-Binol in the right position for reaching higher *ee* values for asymmetric catalysis. The fact that NS(a) is more enantioselective than the homogeneous catalyst clearly suggests the positive effect of the ordered pore wall structure on the enantioselectivity of (R)-(+)-Binol bridging in the network. (R)-(+)-Binol on G-NS is more flexible than that on NS(a) and NS. The lower *ee* value of G-NS compared with that of NS(a) and NS further confirms the above conclusion that the more ordered and rigid pore wall structure favors higher enantioselectivity of the chiral PMOs.

Choosing NS(a) as a model material, the influence of Ti/Binol on the catalytic performance was investigated in the Ti-promoted asymmetric addition of diethylzinc to benzaldehyde (Table 3). With the molar ratio of Ti/Binol in the

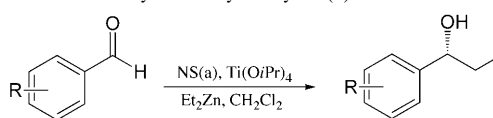Table 3. Influence of Ti/Binol molar ratio on the catalytic properties of NS(a).[a]

Entry	Ti/Binol [mmol mm^{-1}]	Conversion [%]	*ee* [%]
1	6.5	54	90
2	9.5	74	92
3	13	99	94
4	20	99	94

[a] All reactions were carried out in CH$_2$Cl$_2$ with Et$_2$Zn (3.0 mmol) and benzaldehyde (1.0 mmol) for 2 h at 0°C. Conversions and *ee* values were determined by GC on an HP-Chiral 19091G-B213 capillary column.

range of 6.5 to 20, the *ee* value varies from 90 to 94%, thus showing that the Ti/Binol ratio has only a slight influence on the enantioselectivity. A sharp increase of activity is observed upon increasing the Ti/Binol molar ratio. When the Ti/Binol molar ratio exceeds 13, further increasing of this ratio does not influence the performance of the material.

Different kinds of aromatic aldehydes could be converted into the corresponding secondary alcohols on NS(a) with excellent conversions (72–99%) and enantioselectivity (71–94%); all reactions were carried out in CH$_2$Cl$_2$ at 0°C for 2 h (Table 4). Among all the aromatic aldehydes investigated, benzaldehyde shows the highest *ee* value of 94%. The aldehyde with a bulky isopropyl group resulted in a higher *ee* value than that with a smaller CH$_3$ group (entries 2 and 3, Table 4). The substrate with electron-donating CH$_3$ shows a higher *ee* value than those with electron-withdrawing Cl and F (entries 6–8, Table 4), which suggests that the electronic properties of the substituent have a large influence on the *ee* value.

The reusability of NS(a) was investigated in the Ti-promoted asymmetric addition of diethylzinc to benzaldehyde. Within 2 h, only 31% conversion with 53% *ee* was obtained

Table 4. Ti-promoted asymmetric addition of diethylzinc to different kinds of aromatic aldehydes catalyzed by NS(a).[a]

Entry	R-	Conversion [%]	ee [%]
1	H-	99	94
2	4-CH$_3$-	72	82
3	4-CH$_3$CH(CH$_3$)-	93	92
4	4-CH$_3$O-	94	91
5	3-CH$_3$O-	90	92
6	2-CH$_3$-	93	91
7	2-F-	99	81
8	2-Cl-	88	71

[a] All reactions were carried out in CH$_2$Cl$_2$ with Ti(OiPr)$_4$ (1.5 mmol), Et$_2$Zn (3.0 mmol), and aldehyde (1.0 mmol) for 2 h at 0°C. The molar ratio of Ti to ligand was 13. Conversions and *ee* values were determined by GC on an HP-Chiral 19091G-B213 capillary column.

on the reused catalyst, which is much lower than that obtained on the fresh catalyst (99% conversion with 94% *ee*). A previous report shows that the addition of diethylzinc to benzaldehyde is a stoichiometric reaction for benzaldehyde and Ti(OiPr)$_4$.[28] The low activity and *ee* value of the reused catalyst are probably due to the decreased Ti/Binol molar ratio (no Ti(OiPr)$_4$ was added for the recycling reaction) and loss of mesostructural order of the catalyst (see the Supporting Information).

Conclusion

(*R*)-(+)-Binol-functionalized chiral mesoporous organosilica spheres with different pore structures have been successfully synthesized in basic medium. Nanospheres with 2D hexagonal mesostructure and bulk particles with wormhole-like structure were obtained by using low H$_2$O/Si and high H$_2$O/Si ratios in NaOH solution, respectively. Hydrothermal treatment favors the formation of highly ordered 2D hexagonal channels penetrating throughout the nanospheres. Nanospheres with radiative 2D hexagonal channels can be obtained in ammonia solution. The catalysis results show that the nanospheres with highly ordered 2D hexagonal mesostructure are more enantioselective and catalytically active than those with a wormhole-like mesostructure, which suggests that the ordered mesostructure of the chiral PMOs is one of the important factors for achieving high catalytic performance in asymmetric catalysis. Our results also indicate that the co-condensation method is more efficient than the grafting method in view of the uniform coverage of organic moiety, catalytic activity, and enantioselectivity. Through finely controlling the morphology and the mesostructure, efficient chiral PMO catalysts for asymmetric catalysis could be synthesized.

Experimental Section

Chemicals and reagents: Diethylzinc (Et$_2$Zn, 1 M in hexane) was purchased from Sigma–Aldrich Company (USA). Ti(OiPr)$_4$ was purchased from Alfa–Aesar (USA) and was distilled before use. Cetyltrimethylammonium bromide (CTAB), benzaldehyde, and other aldehydes were purchased from Acros Company (USA). (*R*)-(+)-Binol was obtained from Lianyungang Chiral Chemicals Company (China). 3-Chloropropyltrimethoxysilane was obtained from Wuhan Tianmu Science & Technology Development Co. Ltd. (China). Other reagents were purchased from Shanghai Chemical Reagent Incorporation of the Chinese Medicine Group. All solvents were of analytical quality and dried by standard methods. All the reactions were carried out under an argon atmosphere by using standard Schlenk techniques. (*R*)-2,2′-Di(methoxymethyl)oxy-6,6′-di(1-propyltrimethoxysilyl)-1,1′-binaphthyl (BSBinol) was synthesized according to a previous report.[19]

Synthesis of irregularly shaped bulk chiral mesoporous organosilica with (*R*)-(+)-Binol in the framework (Bulk): A mixture (8.5 mmol of Si) of TEOS (1.42 g, 6.8 mmol) and BSBinol (0.596 g, 0.85 mmol) in acetone (2.0 g) was added to an aqueous solution containing CTAB (0.36 g), NaOH (0.08 g), and deionized water (9 g) at 30°C (pH 13.3). After stirring for 12 h at 30°C, the reaction mixture was transferred into a Teflon-lined autoclave and aged at 110°C under static conditions for 72 h. After filtration, the powder product was washed thoroughly with deionized water and dried at 80°C overnight. The molar composition of the reagents was CTAB/NaOH/Si/H$_2$O = 1.0:1.9:8.5:500. The surfactant was extracted by stirring as-synthesized material (1 g) in ethanol (200 mL) containing 12 M HCl (2.0 g) at 80°C for 24 h. The protecting group was removed at the same time. After filtration, the powder was dried at 80°C overnight. The material is denoted as Bulk, which means the material with bulk morphology.

Synthesis of chiral mesoporous organosilica nanospheres in NaOH solution (NS′ and NS): In a typical synthesis, CTAB (0.20 g) was dissolved in deionized water (96 g) under stirring at room temperature. Then NaOH (2 M, 0.70 mL) was added to the solution (pH 12). The temperature of the solution was raised to 80°C. To this clear solution, a mixture of TEOS (1.0 g, 4.8 mmol) and BSBinol (0.4 g, 0.57 mmol) in acetone (2.0 g) was added sequentially and rapidly by injection. After stirring for an additional 2 h, the reaction mixture was filtered directly or transferred into a Teflon-lined autoclave and aged at 110°C under static conditions for 72 h. After filtration, the powder product was washed thoroughly with deionized water and dried at 80°C overnight. The molar composition of the reagents was CTAB/NaOH/Si/H$_2$O = 1:2.6:10.8:9700. The removal of surfactant and protecting group was the same as that for Bulk material. The materials are denoted as NS′ and NS, respectively, where NS′ refers to the nanosphere without hydrothermal treatment and NS refers to the nanosphere with hydrothermal treatment.

Synthesis of chiral mesoporous organosilica nanospheres in ammonia solution (NS(a)): In a typical synthesis, CTAB (0.44 g) was dissolved in deionized water (16.5 g), NH$_3$·H$_2$O (25 wt%, 5.4 g), and EtOH (2.0 g) at room temperature (pH 12.7). A mixture of TEOS (1.66 g, 8 mmol) and BSBinol (0.70 g, 1 mmol) in ethanol (2.6 g) and acetone (2.0 g) was added to the above solution. After stirring at room temperature for 24 h, the reaction mixture was transferred into a Teflon-lined autoclave and aged at 80°C under static conditions for 48 h. After filtration, the powder product was washed thoroughly with deionized water and dried at 80°C overnight. The molar composition of the reagents was CTAB/NH$_3$·H$_2$O/Si/H$_2$O/EtOH = 1:66.7:8.3:950:83.3. The removal of surfactant and protecting group was the same as that for Bulk material. The materials are denoted as NS(a), where "a" refers to the nanosphere synthesized in ammonia.

Grafting BSBinol onto mesoporous silica nanospheres (G-NS): The synthesis of mesoporous silica nanospheres as a support for grafting was the same as that of NS(a) except that TEOS was used as the only silica source. The silica nanospheres (1.0 g) were suspended in DMF (20 mL) containing BSBinol (2.0 mmol) and pyridine (2.0 mL). The mixture was stirred for 24 h at 100°C under an argon atmosphere. The solid material was recovered by filtration, and washed with DMF and acetone sequen-

tially. For removal of the protecting groups, the material (0.5 g) was stirred in ethanol (100 mL) containing 12 M HCl (1.0 g) at 80°C for 24 h. After filtration, the product was dried at 40°C under vacuum overnight. The material was denoted as G-NS.

Characterization: XRD patterns were recorded on a Rigaku RINT D/Max-2500 powder diffraction system by using $Cu_{K\alpha}$ radiation. Nitrogen sorption experiments were performed at −196°C on an ASAP 2020 system. The samples were outgassed at 120°C for 5 h before the measurement. The BET surface area was evaluated from the data in the relative pressure range P/P_0 of 0.05 to 0.25. The total pore volume was estimated from the amount adsorbed at the P/P_0 value of 0.99. The pore diameter was determined from the adsorption branch by the BJH method. Transmission electron microscopy (TEM) was performed with an FEI Tecnai G2 Spirit instrument at an acceleration voltage of 120 kV. STEM and EDX were performed with HRTEM (Philips Tecnai G220 microscope operating at 300 kV). Scanning electron microscopy (SEM) was undertaken on a JEOL JSM-6360 scanning electron microscope operating at an acceleration voltage of 20–30 kV. Solid-state ^{13}C (100.5 MHz) CP/MAS NMR and solid-state ^{29}Si (79.4 MHz) MAS NMR experiments were recorded on a Varian infinity-plus 400 spectrometer equipped with a magic-angle spin probe in a 4 mm ZrO_2 rotor. The experimental parameters for ^{13}C CP/MAS NMR experiments were 10 kHz spin rate, 2 s pulse delay, 6 min contact time, and 1000–2000 scans, and for ^{29}Si MAS NMR experiments were 8 kHz spin rate, 4 s pulse delay, 10 min contact time, and 3000–5000 scans. Infrared spectra were recorded on a Thermo Nicolet Nexus 470 FTIR spectrometer. C, H, and N elemental analysis was performed on a varioEL III apparatus. CD spectra were recorded on a dual-beam DSM 1000 CD spectrophotometer (Olis, Bogart, GA) with a 10 mm quartz cell. Each measurement was the average of five repeated scans recorded from 220 to 350 nm at room temperature (about 25°C). The scanning rate ($nm\,min^{-1}$) was automatically selected by the Olis software as a function of the signal intensity to optimize data collection.

Catalytic reaction: The catalytic properties of (R)-(+)-Binol-functionalized mesoporous materials were investigated in the Ti-promoted asymmetric addition of diethylzinc to aldehydes. After drying under vacuum at 120°C for 3 h, (R)-(+)-Binol-functionalized mesoporous material was stirred in CH_2Cl_2 (4 mL) containing $Ti(OiPr)_4$ (1.5 mmol) at room temperature for 2 h under an argon atmosphere. After addition of Et_2Zn (1 M solution in hexane, 3.0 mmol), the mixture was cooled to 0°C, followed by dropwise addition of aldehyde (1.0 mmol). The reaction mixture was stirred at 0°C. An aliquot (0.5 mL) was taken out by syringe at the desired time and was mixed with saturated NH_4Cl solution (1.0 mL) to stop the reaction. The solid was isolated by filtration and washed with CH_2Cl_2. The organic layer was separated from the filtrate and dried over anhydrous Na_2SO_4. The yield and *ee* value of the product were measured on an Agilent 6890 gas chromatograph equipped with a flame ionization detector and an HP-Chiral 19091G-B213 capillary column (30 m × 0.32 mm × 0.25 μm).

Recycling of the material: After the catalytic reaction, the catalyst was separated by centrifugation and washed with CH_2Cl_2 several times. Then the reactants, benzaldehyde and diethylzinc, and the solvent CH_2Cl_2 were added to the reused catalyst similar to the process described above without addition of $Ti(OiPr)_4$.

Acknowledgements

[1] J. Lei, J. Fan, C. Z. Yu, L. Y. Zhang, S. Y. Jiang, B. Tu, D. Y. Zhao, *Microporous Mesoporous Mater.* **2004**, *73*, 121–128.

[2] a) S. Z. Qiao, H. Djojoputro, Q. H. Hu, G. Q. Lu, *Prog. Solid State Chem.* **2006**, *34*, 249–256; b) J. Y. Ying, C. P. Mehnert, M. S. Wong, *Angew. Chem.* **1999**, *111*, 58–82; *Angew. Chem. Int. Ed.* **1999**, *38*, 56–77.

[3] K. Möller, J. Kobler, T. Bein, *Adv. Funct. Mater.* **2007**, *17*, 605–612.

[4] a) Y. F. Lu, R. Ganguli, C. A. Drewien, M. T. Anderson, C. J. Brinker, W. L. Gong, Y. X. Guo, H. Soyez, B. Dunn, M. H. Huang, J. I. Zink, *Nature* **1997**, *389*, 364–368; b) D. Y. Zhao, P. D. Yang, D. I. Margolese, B. F. Chmelka, G. D. Stucky, *Chem. Commun.* **1998**, 2499–2500.

[5] a) H. Djojoputro, X. F. Zhou, S. Z. Qiao, L. Z. Wang, C. Z. Yu, G. Q. Lu, *J. Am. Chem. Soc.* **2006**, *128*, 6320–6321; b) J. Liu, Q. Yang, L. Zhang, H. Yang, J. Gao, C. Li, *Chem. Mater.* **2008**, *20*, 4268–4275; c) S. Schacht, Q. Huo, I. G. VoigtMartin, G. D. Stucky, F. Schuth, *Science* **1996**, *273*, 768–771; d) S. Z. Qiao, C. X. Lin, Y. Jin, Z. Li, Z. Yan, Z. Hao, Y. Huang, G. Q. Lu, *J. Phys. Chem. A* **2009**, *113*, 8673–8682; e) L. Zhang, S. Z. Qiao, Y. Jin, Z. Chen, H. Gu, G. Q. Lu, *Adv. Mater.* **2008**, *20*, 805–809.

[6] H. P. Lin, C. Y. Mou, *Science* **1996**, *273*, 765–768.

[7] a) P. Schmidt-Winkel, P. D. Yang, D. I. Margolese, B. F. Chmelka, G. D. Stucky, *Adv. Mater.* **1999**, *11*, 303–307; b) H. Zhang, J. M. Sun, D. Ma, X. H. Bao, A. Klein-Hoffmann, G. Weinberg, D. S. Su, R. Schlogl, *J. Am. Chem. Soc.* **2004**, *126*, 7440–7441; c) S. Z. Qiao, C. Z. Yu, Q. H. Hu a, Y. G. Jin, X. F. Zhou, X. S. Zhao, G. Q. Lu, *Microporous Mesoporous Mater.* **2006**, *91*, 59–69.

[8] J. Babin, J. Iapichella, B. Lefevre, C. Biolley, J. P. Bellat, F. Fajula, A. Galarneau, *New J. Chem.* **2007**, *31*, 1907–1917.

[9] H. Zhong, G. R. Zhu, J. Yang, P. Y. Wang, Q. H. Yang, *Microporous Mesoporous Mater.* **2007**, *100*, 259–267.

[10] a) L. Zhang, S. Z. Qiao, Y. G. Jin, L. N. Cheng, Z. F. Yan, G. Q. Lu, *Adv. Funct. Mater.* **2008**, *18*, 3834–3842; b) S. Che, Z. Liu, T. Ohsuna, K. Sakamoto, O. Terasaki, T. Tatsumi, *Nature* **2004**, *429*, 281–284; c) Y. Han, L. Zhao, J. Y. Ying, *Adv. Mater.* **2007**, *19*, 2454–2459; d) B. Wang, C. Chi, W. Shan, Y. H. Zhang, N. Ren, W. L. Yang, Y. Tang, *Angew. Chem.* **2006**, *118*, 2142–2144; *Angew. Chem. Int. Ed.* **2006**, *45*, 2088–2090; e) S. Yang, L. Z. Zhao, C. Z. Yu, X. F. Zhou, J. W. Tang, P. Yuan, D. Y. Chen, D. Y. Zhao, *J. Am. Chem. Soc.* **2006**, *128*, 10460–10466.

[11] a) R. K. Rana, Y. Mastai, A. Gedanken, *Adv. Mater.* **2002**, *14*, 1414–1418; b) H. N. Wang, X. F. Zhou, M. H. Yu, Y. H. Wang, L. Han, J. Zhang, P. Yuan, G. Auchterlonie, J. Zou, C. Z. Yu, *J. Am. Chem. Soc.* **2006**, *128*, 15992–15993.

[12] W. R. Cho, B. J. Cha, H. I. Lee, J. M. Kim, K. Char, *J. Mater. Chem.* **2008**, *18*, 4971–4976.

[13] A. B. D. Nandiyanto, S. G. Kim, F. Iskandar, K. Okuyama, *Microporous Mesoporous Mater.* **2009**, *120*, 447–453.

[14] F. Hoffmann, M. Cornelius, J. Morell, M. Froba, *Angew. Chem.* **2006**, *118*, 3290–3328; *Angew. Chem. Int. Ed.* **2006**, *45*, 3216–3251.

[15] a) C. Baleizao, B. Gigante, D. Das, M. Alvaro, H. Garcia, A. Corma, *Chem. Commun.* **2003**, 1860–1861; b) C. Baleizao, B. Gigante, D. Das, M. Alvaro, H. Garcia, A. Corma, *J. Catal.* **2004**, *223*, 106–113.

[16] a) M. Alvaro, M. Benitez, D. Das, B. Ferrer, H. Garcia, *Chem. Mater.* **2004**, *16*, 2222–2228; b) M. Benitez, G. Bringmann, M. Dreyer, H. Garcia, H. Ihmels, M. Waidelich, K. Wissel, *J. Org. Chem.* **2005**, *70*, 2315–2321; c) D. M. Jiang, Q. H. Yang, H. Wang, G. R. Zhu, J. Yang, C. Li, *J. Catal.* **2006**, *239*, 65–73.

[17] a) R. A. García, R. van Grieken, J. Iglesias, V. Morales, D. Gordillo, *Chem. Mater.* **2008**, *20*, 2964–2971; b) L. Zhang, J. Liu, J. Yang, Q. H. Yang, C. Li, *Chem. Asian J.* **2008**, *3*, 1842–1849.

[18] a) H. T. Chen, S. Huh, J. W. Wiench, M. Pruski, V. S. Y. Lin, *J. Am. Chem. Soc.* **2005**, *127*, 13305–13311; b) S. Huh, H. T. Chen, J. W. Wiench, M. Pruski, V. S. Y. Lin, *J. Am. Chem. Soc.* **2004**, *126*, 1010–1011.

[19] X. Liu, P. Y. Wang, Y. Yang, P. Wang, Q. Yang, *Chem. Asian J.* **2010**, *5*, 1232–1239.

[20] J. Liu, L. Zhang, Q. H. Yang, C. Li, *Microporous Mesoporous Mater.* **2008**, *116*, 330–338.

[21] Q. Cai, Z. S. Luo, W. Q. Pang, Y. W. Fan, X. H. Chen, F. Z. Cui, *Chem. Mater.* **2001**, *13*, 258–263.

[22] D. Y. Zhao, Q. S. Huo, J. L. Feng, B. F. Chmelka, G. D. Stucky, *J. Am. Chem. Soc.* **1998**, *120*, 6024–6036.

[23] Y. S. Lin, C. P. Tsai, H. Y. Huang, C. T. Kuo, Y. Hung, D. M. Huang, Y. C. Chen, C. Y. Mou, *Chem. Mater.* **2005**, *17*, 4570–4573.

[24] D. M. Jiang, Q. H. Yang, J. Yang, L. Zhang, G. R. Zhu, W. G. Su, C. Li, *Chem. Mater.* **2005**, *17*, 6154–6160.

[25] a) K. Pathak, I. Ahmad, S. H. R. Abdi, R. I. Kureshy, N. U. H. Khan, R. V. Jasra, *J. Mol. Catal. A* **2008**, *280*, 106–114; b) H. M. Wang, Z. Wang, K. L. Ding, *Tetrahedron Lett.* **2009**, *50*, 2200–2203; c) X. S. Wang, X. W. Wang, H. C. Guo, Z. Wang, K. L. Ding, *Chem. Eur. J.* **2005**, *11*, 4078–4088.

[26] D. J. Mihalcik, W. B. Lin, *Angew. Chem.* **2008**, *120*, 6325–6328; *Angew. Chem. Int. Ed.* **2008**, *47*, 6229–6232.

[27] Z. G. Zhang, H. Qian, J. Longmire, X. M. Zhang, *J. Org. Chem.* **2000**, *65*, 6223–6226.

[28] M. Mori, T. Nakai, *Tetrahedron Lett.* **1997**, *38*, 6233–6236.